SCIENTIFIC REPORTS

OPEN

SUBJECT AREAS:
CHEMOTHERAPY
DRUG DELIVERY
CELL-CYCLE EXIT

Received
8 October 2013

Accepted
12 March 2014

Published
27 March 2014

Correspondence and requests for materials should be addressed to Q.H. (qinhe@scu.edu.cn)

Pretreatment with chemotherapeutics for enhanced nanoparticles accumulation in tumor: the potential role of G2 cycle retention effect

Huile Gao[1], Guanlian Hu[1], Qianyu Zhang[1], Shuang Zhang[2], Xinguo Jiang[2] & Qin He[1]

[1]Key Laboratory of Drug Targeting and Drug Delivery Systems, West China School of Pharmacy, Sichuan University; No.17 Block 3, Southern Renmin Road, Chengdu, 610041, China, [2]Key Laboratory of Smart Drug Delivery (Fudan University), Ministry of Education; School of Pharmacy, Fudan University; 826 Zhangheng Road, Shanghai, 201203, China.

Ligands were anchored onto nanoparticles (NPs) to improve the cell internalization and tumor localization of chemotherapeutics. However, the clinical application was shadowed by the complex preparation procedure and the immunogenicity and poor selectivity and stability of ligands. In this study, a novel strategy was developed to elevate the tumor cellular uptake and tumor localization of NPs utilizing the G2/M phase retention effect of docetaxel, one of the most common chemotherapeutics. Results showed pretreatment with docetaxel could effectively arrest cells in G2/M phase, leading to an enhanced cell uptake of NPs, which may be caused by the facilitated endocytosis of NPs. In vivo imaging and slice distribution also demonstrated the pretreatment with docetaxel improved the localization of NPs in tumor. This strategy can be easily transferred to clinical for cancer management. Combination chemotherapeutics injections with commercial nano-drugs may result in better antitumor effect than the administration of a single drug.

Cancer is still the most serious threat for human beings[1]. Although chemotherapy is one of the most common methods for controlling the cancer, the application is shadowed by poor clinical outcome and the serious side effects which were owing to undesired systemic distribution[2]. Nanoparticles (NPs), including liposomes, micelles and dendrimers, have been used as carriers to deliver chemotherapeutics into tumors based on enhanced permeability and retention (EPR) effect[2–7]. Although the side effect is reduced, tumor targeting effect is far from sufficient because of the non-optimal pharmacokinetics and existence of several physiological barriers that led to heterogeneous distribution in cancer[8].

Many ligands have been used for improving tumor targeting delivery, including proteins, peptide, aptamers and small molecular compounds, which were based on the specific interaction between ligands and receptors/carriers or the unspecific interaction between ligands and cell membranes[9–13]. Although lots of researches have been published and several candidates are under clinical evaluation, the application of this strategy is restricted by the complex preparation methods as well as the immunogenicity and poor stability of ligands. Importantly, there were controversies as to the function of ligand modification; some researched showed ligand-modification improved the tumor localization while some showed not[14–17]. Additionally, the clinical outcome of nanomedicines was far from perfect. There is a need to develop a more convenient and effective method for enhancing targeting delivery efficiency.

It was known that the uptake of NPs by cells was influenced by not only the size and surface properties of NPs but also the difference in cell cycle phases[18–22].Normally, cell cycle possesses five phases: G0, G1, S, G2 and M phase. The uptake ability could be ranked according to following sequence: G2/M > S > G0/G1[22]. Based on the above knowledge, it may be useful to arrest cells in G2/M phase to improve the NPs uptake. Many chemotherapeutics could affect the cell cycle distribution. For example, docetaxel (DTX) and paclitaxel could arrest the cells in G2/M phase[23]. In addition, DTX was widely used in clinical for the treatment of various cancers[23–25]. Thus this study utilized the G2/M phase retention effect of docetaxel for enhanced tumor delivery of NPs.

In this study, different fluorescent probes were used to label poly(ethyleneglycol)-poly(ε-caprolactone) NPs. Fluorescein isothiocyanate-conjugated NPs (FITC-NPs) was used in *in vitro* study to determine the effect of DTX on cellular uptake. For *in vivo* evaluation, a near-infrary dye, DiR, was loaded into NPs (DiR-NPs). Cell cycles

were stained to determine the uptake ability of cells in different cycles. Subcellular localization and uptake mechanism was determined to elucidate the potential uptake pathway of NPs by cells after DTX pretreatment.

Results

NP characterization. The mean particle sizes, polydispersity index (PDI) and zeta potentials of the FITC-NPs and DiR-NPs were reported in Supplementary Table S1. Particle sizes were about 100 nm and were narrowly distributed. The zeta potentials of FITC-NPs and DiR-NPs were −10.6 mV and −11.2 mV respectively. The morphology of NPs was spherical as demonstrated by transmission electronic microscopy (TEM) (see Supplementary Fig. S1 online).

Cellular uptake. U87 cells (a human glioblastoma cell line) were used for the evaluation of cellular uptake of FITC-NPs. The uptake of FITC-NPs was positively related to the concentration of DTX (Figure 1a). After incubation with 0.01 μg/mL of DTX for 24 h, cellular uptake of FITC-NPs was 1.43-fold as that untreated U87 cells ($P = 0.042$). Increasing the DTX concentration to 0.1 μg/mL could further improve the cell uptake, which was 1.69-fold as that of untreated cells ($P = 0.016$). Correspondingly, the percentage of cells in G2/M phase increased accompany with the increase of DTX concentration (Figure 1b). The increased uptake also showed a concentration dependent manner (Figure 1c). Although pretreating cells with 0.1 μg/mL of DTX could induce more apoptotic cells compared with control, there were still only 3.7% apoptotic cells (2.4% in control cells) (see supplementary Fig. S2 online), suggesting the enhanced uptake was mainly due to the G2/M retention effect rather than apoptotic cells. Treatment with 0.5 μg/mL DTX led to much more apoptotic cells (about 30% ~ 60% according to previous works[26,27]), however, the uptake of NPs by cells treated with 0.5 μg/mL DTX was only 1.2-fold high as that of cells treated with 0.1 μg/mL DTX, further demonstrating that the elevated cell uptake was mainly caused by G2/M retention effect. Pretreating with other chemotherapeutics, such as doxorubicin, paclitaxel, lapatinib and cisplatin also could affect the cellular uptake of FITC-NPs, which was positively related with the percentages of cells in G2/M phase (see supplementary Fig. S3 online). These results suggested that G2/M phase retention of cells could indeed facilitate the uptake of NPs.

Cellular uptake of different cell phases. To further evaluate the role of cell cycle on cellular uptake, cell cycle was stained by kit (Figure 2). At different incubation time, cellular uptake of FITC-NPs at G2/M and S phase was higher than that at G0/G1 phase (Figure 2a, $P = 0.063$ and 0.049 for G2/M and S phase respectively at 2 h incubation), suggesting G2/M and S phase possessed higher ability in taking up NPs. Pre-incubation U87 cells with 0.1 μg/mL DTX could significantly enhance the cell uptake (Figure 1a, $P = 0.016$). Uptake by cells in G2/M an S phase was higher than that in G0/G1 phase ($P = 0.24$ and 0.39 for G2/M and S phase respectively), which was consistent with the above results. However, after cell cycle was stained, it showed the uptake by cells in all phases were higher than that of untreated cells ($P = 0.008$, 0.011 and 0.009 for G2/M, S and G0/G1 phase respectively), suggesting pre-incubation with DTX could facilitate the cellular uptake of NPs. Similar results were observed after incubating U87 cells with FITC-NPs of different concentrations (Figure 2b). These results were consistent with studies performed on A549 cells (a lung carcinoma cell line) (see supplementary Fig. S4 online).

Cell cycle synchronization was also used for evaluating the uptake by cells in different cell cycle phase. FBS-free medium was utilized for G0/G1 phase synchronization, thymidine treatment was utilized for S phase synchronization and nocodazole treatment was utilized for G2/M phase synchronization[28–30]. Cells in G0/G1, S and G2/M phase were increased from 69.1%, 19.9% and 11.0% to 76.9%, 23.9% and 43.0% after synchronization by FBs-free medium, thymidine and nocodazole respectively (Figure 2d). Nocodazole-treated cells showed highest uptake of FITC-NPs, which was 2.05-, 2.11- and 1.21-fold higher than the uptake by control cells, G0/G1-synchronized cells and S-synchronized cells respectively (Figure 2c), strongly demonstrating G2/M and S phase possessed higher ability in taking up NPs.

Internalization of NPs. Endosomes and mitochondria were labeled by LysoTracker and MitoTracker to evaluate the participation of these two organelles in the uptake procedure. After pre-treated with 0.1 μg/mL of DTX, cells were changed into bigger and more spherical form compared to untreated cells (Figure 3), suggesting the cells were under abnormal status. After 15-min incubation, the uptake of FITC-NPs by DTX-treated cells were higher than that by untreated cells (Figure 3a), which was consistent with above results. However, most FITC-NPs were colocalized with endosomes and no difference was observed between DTX-treated cells and untreated cells. After 60-min incubation, although some of NPs were distributed into cytoplasm, most of NPs were still localized in endosomes (Figure 3a), which was consistent with previous results. These results suggested the DTX pretreatment could enhance the uptake of NPs rather than facilitate the escape of NPs from endosomes.

However, the colocalization of NPs with mitochondria was not the same as that with endosomes. After 15-min incubation, there was poor colocalization between NPs and mitochondria in both DTX-treated and untreated cells (Figure 3b). Increasing the incubation time to 60-min could considerably improve the colocalization between NPs and mitochondria. Especially in DTX pre-treated cells, many of NPs were colocalized with mitochondria, which may lead to cytotoxicity to cells. These results indicated the DTX treatment could improve the cell uptake of NPs as well as the cytotoxicity to cells if

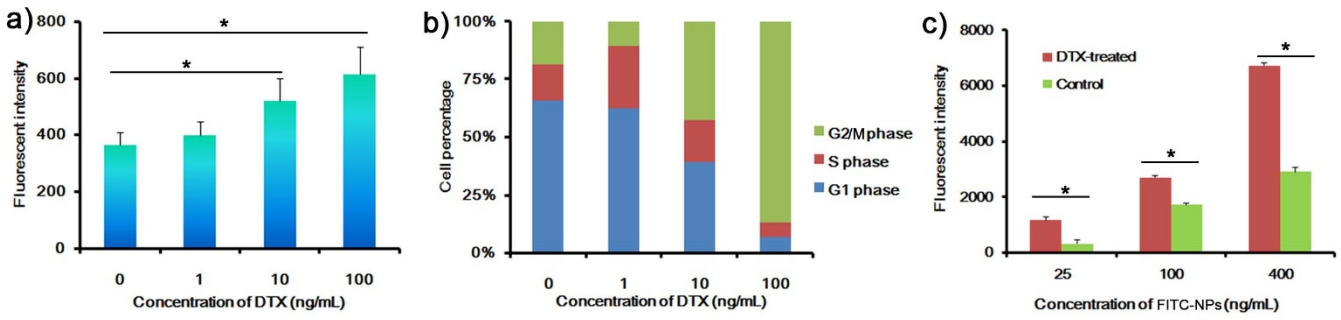

Figure 1 | Effect of DTX on the uptake of FITC-NPs. (a) Cellular uptake of FITC-NPs for 1 h after U87 cells pretreated with different concentrations of DTX for 24 h. (b) Cell cycle distribution of U87 cells treated with different concentrations of DTX for 24 h. (c) Cellular uptake of different concentrations of FITC-NPs for 1 h after U87 cells pretreated with 0 or 0.1 μg/mL of DTX for 24 h. n = 3, $*p < 0.05$.

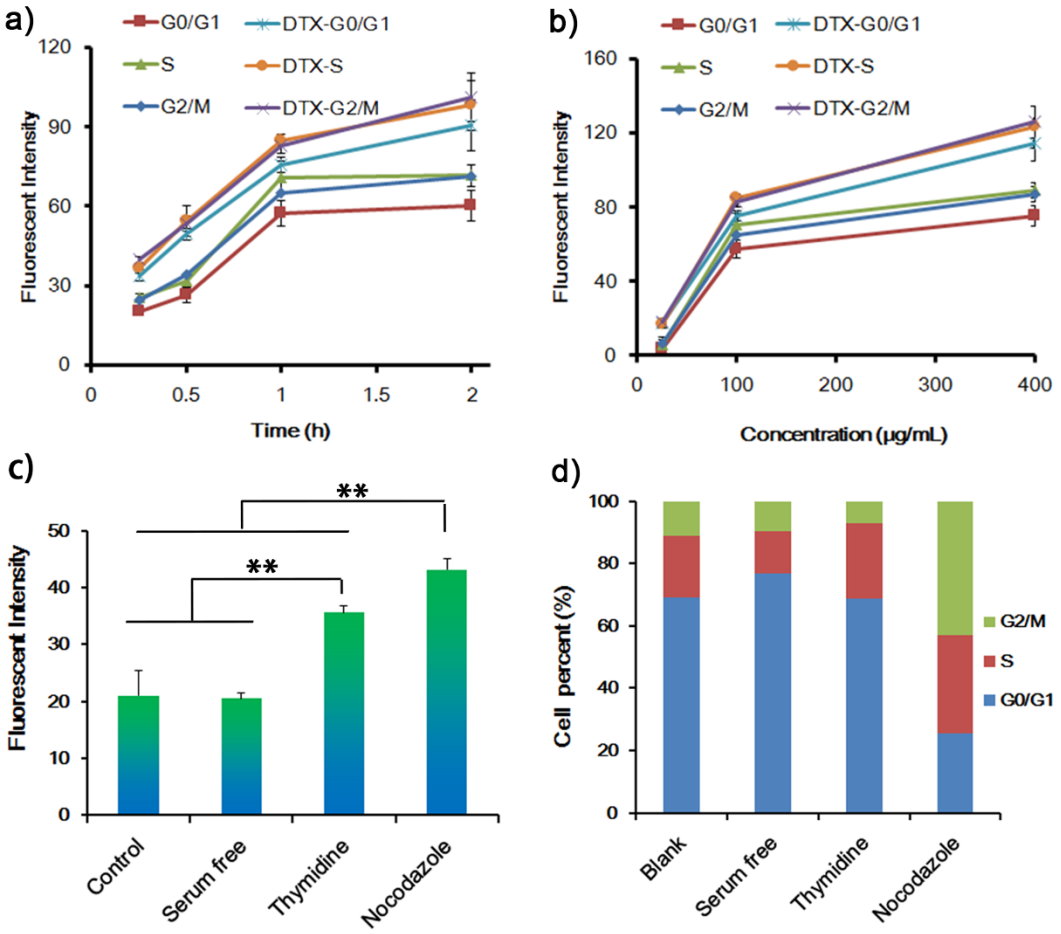

Figure 2 | Cell cycle uptake of FITC-NPs. (a) Different cell cycle uptake of 100 μg/mL of FITC-NPs for vary times after U87 cells pretreated with 0.1 μg/mL of DTX for 24 h. (b) Different cell cycle uptake of different concentrations of FITC-NPs for 1 h after U87 cell pretreated with 0.1 μg/mL of DTX for 24 h. (c) Cell uptake of 100 μg/mL of FITC-NPs for 1 h after cells synchronized by different conditions, no-treated cells were used as control. (d) Cell cycle distribution after synchronized by different conditions, no-treated cells were used as control. **$p < 0.01$. ($n = 3$).

NPs were loaded with chemotherapeutics, which was useful for killing of cancer cells.

Cellular uptake mechanism. Obviously, the uptake of FITC-NPs by both DTX-pretreated and untreated cells was energy-dependent, because the uptake by DTX-pretreated and untreated cells were significantly ($P = 0.0003$ and 0.047 respectively) reduced to 63.69% and 83.71% respectively after energy depletion by sodium azide (Figure 4). Phenylarsine oxide, the endocytosis inhibitor, significantly ($P = 0.00016$ and 0.00013 respectively) decreased the cellular uptake of FITC-NPs by DTX-pretreated and untreated cells to 59.3% and 58.0% respectively, suggesting that endocytosis was involved in the uptake by both cells, which was consistent with previous result[17]. The lysosome inhibitor monensin[31] significantly ($P = 0.033$) inhibited the uptake of FITC-NPs by DTX-pretreated cells rather than untreated cells, suggesting lysosomes played a more important role in uptake by DTX-pretreated cells than that by untreated cells. Filipin, a special inhibitor of caveolae-mediated endocytosis[32], significantly ($P = 0.0023$) decreased the FITC-NPs uptake by untreated cells rather than by DTX-pretreated cells, suggesting caveolae-mediated endocytosis was not considerably involved in the uptake of FITC-NPs by DTX-pretreated cells. Other inhibitors displayed almost the same functions on the uptake by DTX-pretreated cells and untreated cells, suggesting DTX-pretreatment did not alter the uptake mediated by clathrin and macrophage.

***Ex vivo* imaging and tissue distribution.** *Ex vivo* imaging was utilized to determine the tissue distribution of DiR-NPs in U87 xenografts bearing mice pretreated with 20 mg/kg DTX for 24 h or not (Figure 5a). In untreated mice, fluorescent intensity in liver was the highest because liver is the main organ to eliminate exogenous particles, which was consistent with many of previous studies. There was a relatively high intensity in tumor because of the EPR effect, which made NPs passively permeate neovasculature and stay in the tumor site. Pretreatment with DTX could alter the distribution of NPs in mice. The intensity of NPs in tumor was considerably higher than that of untreated mice, which was 1.91-fold as that of untreated mice (Figure 5b), suggesting pretreating with DTX could improve the tumor cellular uptake of NPs, thus leading to a higher accumulation in tumor site, which was consistent with *in vitro* results. However, the distribution in liver was also higher than that of untreated mice (Figure 5b).

To further elucidate the distribution, slices were prepared. Accordingly, the fluorescent intensity in tumor slice of DTX pretreated mice was considerably higher than that of untreated mice (Figure 5c), which was consistent with ex vivo imaging. Although there was higher fluorescent intensity in liver slice of DTX-pretreated mice compared to that of untreated mice, most of fluorescence was distributed in Kuffer cells rather than liver cells. In other words, pretreating with DTX could elevate the uptake by Kuffer cells rather liver cells in liver, suggesting the side effect in liver should be low. In most of other organs, the fluorescent intensity showed no obvious difference between DTX-pretreated mice and untreated mice (Figure 6), indicating DTX-pretreatment did not obviously alter

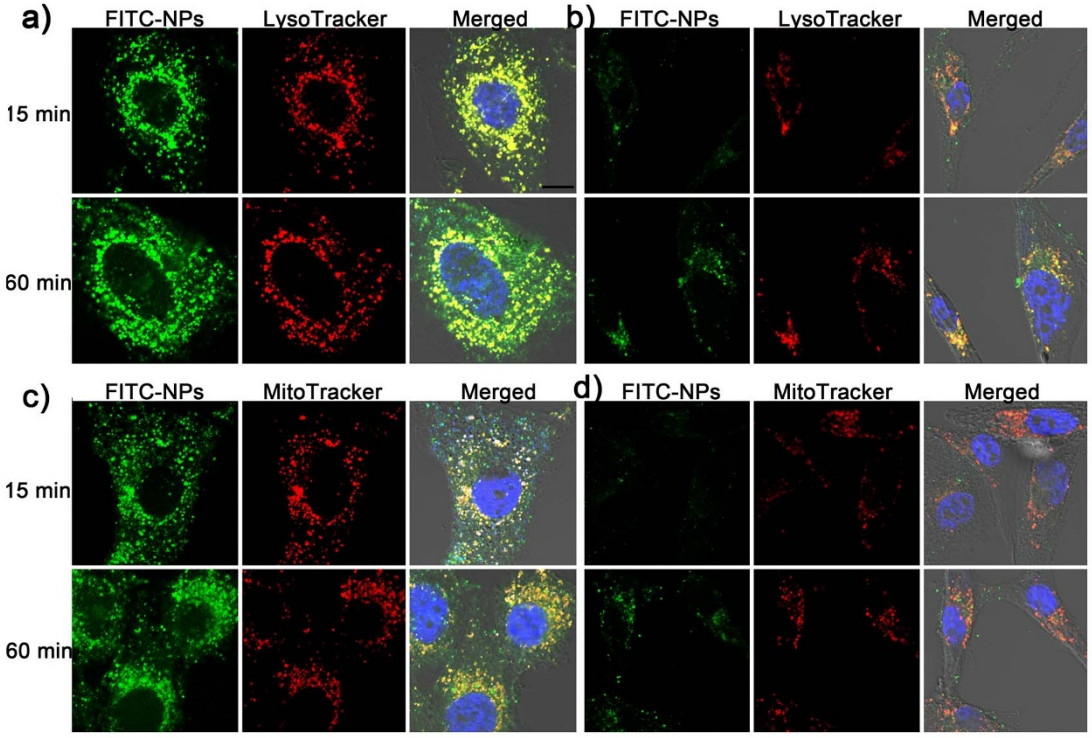

Figure 3 | Subcellular localization of FITC-NPs in U87 cells pretreated or untreated with 0.1 μg/mL of DTX. (a) Subcellular localization of FITC-NPs with endosomes after 15- or 60-min incubation in U87 cells pretreated with 0.1 μg/mL of DTX. (b) Subcellular localization of FITC-NPs with endosomes after 15- or 60-min incubation in untreated U87 cells. (c) Subcellular localization of FITC-NPs with mitochondria after 15- or 60-min incubation in U87 cells pretreated with 0.1 μg/mL of DTX. (d)Subcellular localization of FITC-NPs with mitochondria after 15- or 60-min incubation in untreated U87 cells. Blue represents nuclei that stained by DAPI, green represents FITC-NPs, red represents endosomes (a, b) or mitochondria (c, d), bar represents 10 μm.

the distribution of NPs in normal tissues, which was good news for its future application in cancer treatment.

Discussion

The influence of chemotherapeutics on cell cycle were well known, and many researches focused on developing drugs that directly interacted with cell cycle-related kinases[33,34]. There were rarely studies discussing the potential use of cell cycle in drugs and/or NPs delivery. Recently, Kim et al demonstrated the uptake ability of NPs by cells in different cell cycles were ranked in the following sequence: G2/M > S > G0/G1[22]. The main reason was the difference in incubation time with NPs. Cells in G2/M phase interacted with NPs for the longest time while cells in G0/G1 phase had lest time to endocytose more NPs. Thus arresting cells in G2/M phase could further lead to higher uptake of NPs.

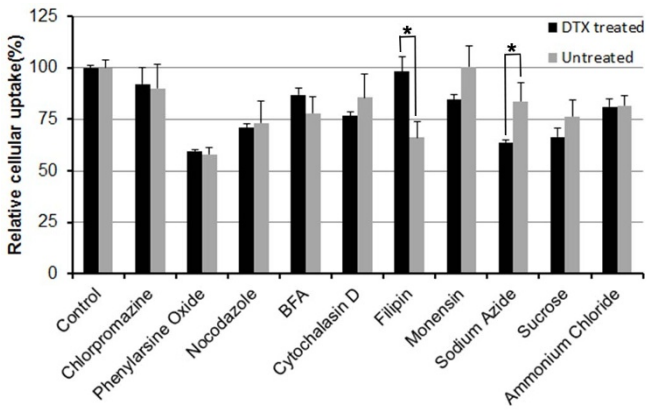

Figure 4 | Uptake mechanism of FITC-NPs by U87 cells pretreated or untreated with 0.1 μg/mL of DTX.

In this study, PEG-PCL NPs were used for evaluation of cellular uptake and *in vivo* distribution. Previous results showed the half lethal dose of PEG-PCL was 1.47 g/kg[35], which was much higher than the concentrations used in this study (200 μg/mL for *in vitro* study and 100 mg/kg for *in vivo* study), thus NPs could not perturb the function of cells. In other words, the change on uptake ability of cells was mainly caused by DTX-pretreatment.

DTX is an anti-microtubule agent that could stabilize the microtubules in cells that led to disfunction of microtubules and retention of cells in G2/M phase[23]. The arrestment in G2/M phase led to higher uptake of NPs which was demonstrated by cellular uptake. However, there may be other mechanisms that were involved in the uptake process, because the uptake ability in all three phases was considerably elevated after DTX-pretreatment, which needed further evaluation. Cell cycle synchronization was also used for evaluating the uptake by cells in different cell cycle phases. After synchronized to G2/M phase, cellular uptake ability was significantly improved compared with G0/G1 and S phase synchronization ($P = 0.0009$ and 0.0068 respectively), suggesting arrestment in G2/M phase may facilitate the cell uptake. However, it could not explain the S phase synchronization elevated the cell uptake without increased G2/M phase distribution.

Microtubules are cytoskeletal proteins that are responsible for mitosis, intracellular transport, cellular intensity and many other functions[36–38]. Microtubules stabilization may disturb the transport of NPs from endosomes to lysosomes[37], making it hard for NPs to escape from endosomes, which is why most NPs were colocalized with endosomes in cells pretreated with DTX. This conclusion could also be supported by the uptake mechanism study, in which lysosome inhibitor considerably reduced the uptake of FITC-NPs by

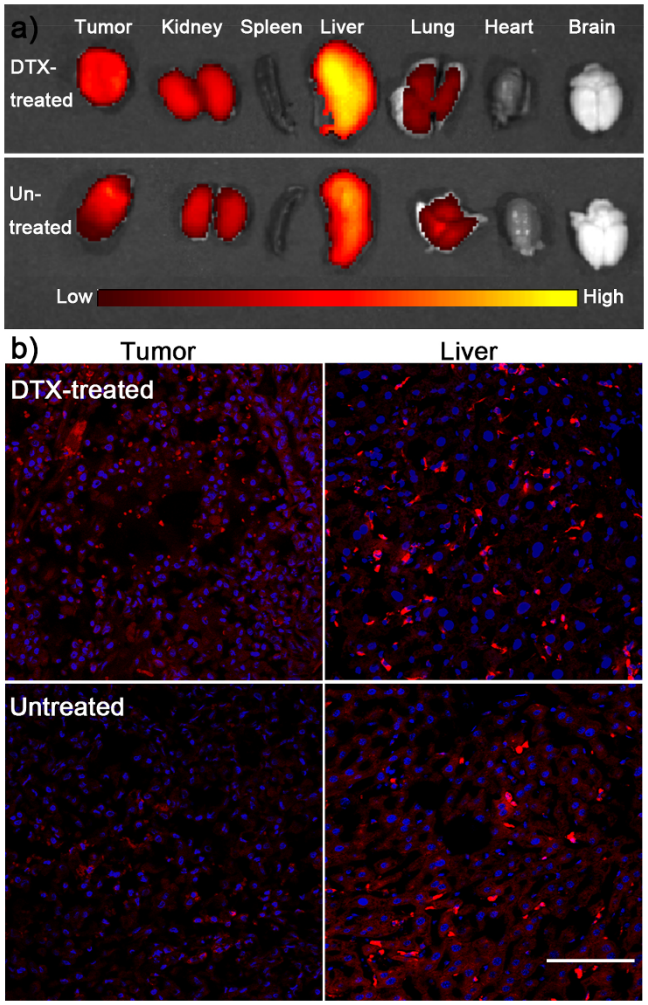

Figure 5 | ***Ex vivo*** **imaging and tissue distribution of DiR-NPs.** (a) *Ex vivo* imaging of organs from DiR-NPs treated mice that pretreated or untreated with 20 mg/kg of DTX. (b) Semi-quantitative of fluorescent intensity in different organs. (c)Fluorescence distribution in tumor and liver from DiR-NPs treated mice that pretreated or untreated with 20 mg/kg of DTX. Bar represents 100 μm.

DTX-pretreated cells. Additionally, low dose of paclitaxel (analog of DTX) could affect the microtubules dynamics[39], which may also contribute to the poor intracellular transport of endosomes. In other words, the transport from endosomes to lysosomes was the main pathway that was involved in the uptake by DTX-pretreated cells. Thus enabling NPs with endosome escape property may be useful for drug delivery to cytoplasm or other organelles. However, it also showed that some of the FITC-NPs were located in cytoplasm of DTX-pretreated cells, suggesting the function of microtubules was not totally erased. Additionally, it was pointed out that cytoplasmic dynein could stimulate early-to-late endosome vesicle fusion[40], which may contribute to the distribution of NPs in cytoplasm.

Normally, mitochondria were protected by membrane and hard to be accessed. However, during certain conditions, such as ischemia, the permeability of membrane of mitochondria increased[41,42]. In this study, DTX is a cytotoxic agent that may possess harmful effect to mitochondria, which led to the increased colocalization of NPs with mitochondria. However, the exact mechanism needed to be explored in future.

In vivo results demonstrated DTX-pretreatment could enhance tumor accumulation of NPs, which was useful for cancer management. Nowadays, several nanoparticulated chemotherapeutics were commercially available, including Doxil, Nab, etc.[6,43]. Clinical results showed most of these nanoparticulated drugs could improve the tolerance rather than antitumor effect[44]. According to this study, researchers or clinicians may pretreat tumor bearing patient with chemotherapeutics followed with nanoparticulated drugs, which may improve accumulation of nanoparticulated drugs in tumors thus leading to elevated antitumor effect. This strategy was convenient and simple for clinical application in that only current available drugs were needed rather than newly-approved drugs.

Additionally, the distribution in most normal tissues was not altered after DTX-pretreatment. However, liver distribution increased after DTX-treatment. After nuclei staining, it showed the increased localization of NPs in liver was caused by the elevated internalization of NPs by Kuffer cells rather than liver cells. It was pointed out that Kuffer cells were central in the removal of NPs from organism[45]. Thus the increased localization in Kuffer cells in liver may not cause serious side effect to liver.

Although this study demonstrated the DTX-pretreatment could be utilized for enhanced NPs delivery to tumors, several aspects needed to be further explored before clinical use. First, the time interval needs to be confirmed. In this study, NPs were administered 24 h after DTX treatment which was based on the experiment that 24 h-incubation could effectively arrest cells in G2/M phase. However, this interval could be optimized to further improve the combination effect. Second, the release of drugs from NPs needs to be optimized to release drugs as much as possible in tumor cells rather than in blood circulation. Third, the combination dose needs to be further determined. In this study, 20 mg/kg was used for *in vivo* study according to the clinical application. If available, an optimized

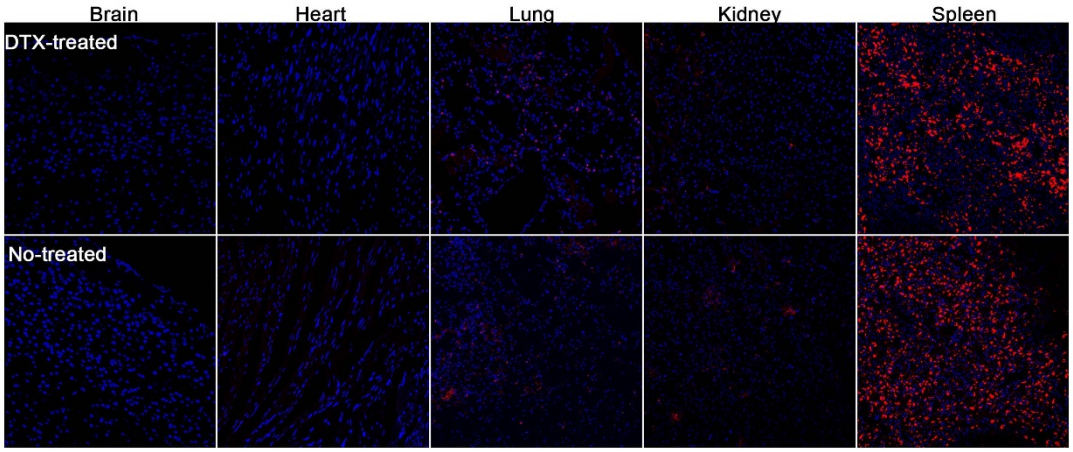

Figure 6 | **Tissue distribution of DiR-NPs treated mice that pretreated or untreated with 20 mg/kg of DTX.** Bar represents 100 μm.

dose should cause the highest localization of NPs in tumor site while leading to the lowest side effect.

In conclusion, pretreating U87 cells with DTX effectively enhanced the uptake ability of NPs, which was positively related with concentrations of DTX. Although cells in G2/M phase showed higher uptake ability compared with cells in other cell cycle phases, the uptake ability of cells in all phases were elevated after DTX pretreatment. Subcellular localization studies demonstrated DTX-pretreatment could facilitate the uptake of NPs but not the escape from endosomes. *In vivo*, pretreated tumor xenografts bearing mice resulted in elevated tumor localization of NPs. Although the distribution of NPs in liver was also increased, most of NPs were located in Kuffer cells.

Methods

Materials. DTX was purchased from Knowshine (Shanghai, China). Methoxy poly(ethyleneglycol)-poly(ε-caprolactone) (MPEG-PCL)(Mw: 3 k–15 k) and FITC-conjugated poly(ethyleneglycol)-poly(ε-caprolactone) (FITC-PEG-PCL)(Mw: 3 k–15 k) were synthesized as previously described[27]. The near infrared dye 1,1′-Dioctadecyl-3,3,3′,3′-tetramethylindotricarbocyanine Iodide (DiR) was purchased from Biotium (Hayward, CA). DAPI was purchased from Beyotime (Haimen, China).U87 and A549 cells were purchased from the Institute of Biochemistry and Cell Biology, Shanghai Institute for Biological Sciences, Chinese Academy of Sciences (Shanghai, China). Plastic cell culture dishes and plates were purchased from Wuxi NEST Biotechnology Co. Ltd. (Wuxi, China). LysoTracker Red, MitoTracker Red, Click iT™ EdU flow cytometry assay kit, Dulbecco's Modified Eagle Medium (high glucose) cell culture medium (DMEM) and FBS were purchased from Life Technologies (Grand Island, NY, USA). All other chemicals were analytical reagent grades and were purchased from Sinopharm Chemical Reagent (Shanghai, China).

BALB/c nude mice (male, 4–5 weeks, 18–22 g) were obtained from the Shanghai Slac Laboratory Animal Co, Ltd. (Shanghai, China) and maintained under standard housing conditions. All animal experiments were carried out in accordance with protocols evaluated and approved by the ethics committee of SIchuan University.

Preparation and characterization of NPs. The PEG-PCL NPs were prepared by a previously described emulsion/solvent evaporation method[46]. Briefly, 30 mg of MPEG-PCL (contained 600 μg of DiR)or 30 mg of FITC-PEG-PCL were dissolved in 1 mL of dichloromethane and then added to 5 mL of a 0.6% sodium cholate hydrate solution before subjected to pulse sonication for 75 s at 200 W on ice using a probe sonicator (Scientz Biotechnology Co. Ltd., China). After the evaporation of dichloromethane, the FITC-NPs and DiR-NPs were condensed to a fixed concentration by ultrafiltration at 4,000 *g*. The particle sizes and Zeta potentials were determined by a Malvern Zeta Sizer (Malvern, NanoZS, UK). The morphology was examined by TEM after staining with 2% (w/v) phosphotungstic acid solution.

Cellular uptake. U87 glioma cells and A549 cells in the logarithmic growth phase were seeded on 12-well plates at a density of 2×10^4 cells/mL. Twenty four hours later, DTX of different concentrations or different chemotherapeutics were added into the wells and incubated for 24 h. After removing the drug-containing culture medium, FITC-NPs of different concentrations were added into wells and incubated for 1 h. After the adsorptive and free particles were removed by washing with ice-cold PBS, cell were harvested and detected by a FACS Aria Cell Sorter (BD, USA). To determine the cell cycle distribution, DTX-treated and untreated cells were harvested, stained with PI and evaluated using a FACS Aria Cell Sorter (BD, USA).

Cell cycle uptake. Cells were seeded and pre-treated with 0.1 μg/mL of DTX for 24 h as described above. After removing the DTX-contained culture medium, 10 μmol/L Click iT™ EdU was added into wells before different concentrations of FITC-NPs were added into wells and incubated for different periods of time. After washed with ice-cold PBS and harvested, cells were stained according to the manual of Click iT™ EdU flow cytometry assay kit. The FITC intensity of cells in different cell cycle phases were detected by a FACS Aria Cell Sorter (BD, USA). For synchronization, cells were seeded into 6-well plates and pretreated with FBS-free medium, 4 mM thymidine or 0.8 μg/mL nocodazole for 24 h. Then 100 μg/mL FITC-NPs in fresh medium were added into wells and incubated for 1 h. After washed, cells were harvested for fluorescent intensity detection using a FACS Aria Cell Sorter (BD, USA).

Intracellular localization. U87 cells were seeded in glass-bottom dishes at a density of 1×10^4 cells/mL and incubated at 37°C for 24 h. After pre-incubating with 0 or 0.1 μg/mL of DTX for 24 h, the cells were treated for 15 min or 60 min with 100 μg/mL FITC-NPs. Thirty minutes before the incubation stopped, cells were added with LysoTracker Red DND-99 (50 nmol/L, a marker of endolysosomal compartments) or MitoTracker Red (50 nmol/L, a marker of mitochondria). After nuclei staining with DAPI (1 μg/mL) for 5 min, the cells were washed, fixed and mounted in fluorescent mounting medium. Images were captured with a confocal microscope (TCS SP5, Leica, Germany) and were superimposed to determine the intracellular localization of the FITC-NPs.

Cellular uptake mechanism. U87 cells were seeded in 12-well plates at a density of 2×10^5 cells/mL and incubated for 24 h followed with a 24 h of incubation with 0 or 0.1 μg/mL of DTX. After a 20-min pre-incubation in DMEM, the cells were treated with 100 μg/mL of FITC-NPs and various inhibitors for 1 h: PBS (control), 20 μg/mL chlorpromazine, 2 μmol/L phenylarsine oxide, 10 μg/mL filipin, 40 μmol/L cytochalasin D, 450 mmol/L sucrose, 0.1% w/v sodium azide, 200 nmol/L monensin, 50 μmol/L nacodazole, 20 μg/mL BFA. After washing with ice-cold PBS, the cells were digested and the mean fluorescence intensity was observed by flow cytometry (FACS Aria Cell Sorter, BD, USA).

***Ex vivo* imaging and tissue distribution.** U87 xenografts bearing mice were established through subcutaneous injection of 5×10^6 U87 cells. Twenty-four hours after pre-injecting through tail vein with saline or 10 mg/kg of DTX, DiR-NPs were *i.v.* injected into U87 xenografts bearing mice. The distribution of fluorescence was observed by an IVIS spectrum *in vivo* imaging system (Caliper, MA, USA) 2 h post injection. Mice were sacrificed at 2 h and the *ex vivo* image of the brain was also captured at that time. Tissues were applied to slices preparation and nuclei were stained by 1 μg/mL of DAPI for 5 min. The distribution of fluorescence was observed using a confocal microscope (Olympus, Japan).

1. Siegel, R., Naishadham, D. & Jemal, A. Cancer statistics, 2013. *CA Cancer J Clin* **63**, 11–30 (2013).
2. Lammers, T., Kiessling, F., Hennink, W. E. & Storm, G. Drug targeting to tumors: principles, pitfalls and (pre-) clinical progress. *J. Control. Release* **161**, 175–87 (2012).
3. Lammers, T., Hennink, W. E. & Storm, G. Tumour-targeted nanomedicines: principles and practice. *Br J Cancer* **99**, 392–7 (2008).
4. Matsumura, Y. & Maeda, H. A new concept for macromolecular therapeutics in cancer chemotherapy: mechanism of tumoritropic accumulation of proteins and the antitumor agent smancs. *Cancer Res.* **46**, 6387–92 (1986).
5. Fang, J., Nakamura, H. & Maeda, H. The EPR effect: Unique features of tumor blood vessels for drug delivery, factors involved, and limitations and augmentation of the effect. *Adv Drug Deliv Rev* **63**, 136–51 (2011).
6. Barenholz, Y. C. Doxil(R) - The first FDA-approved nano-drug: Lessons learned. *J. Control. Release* **160**, 117–34 (2012).
7. Maeda, H., Nakamura, H. & Fang, J. The EPR effect for macromolecular drug delivery to solid tumors: Improvement of tumor uptake, lowering of systemic toxicity, and distinct tumor imaging in vivo. *Adv Drug Deliv Rev* **65**, 71–9 (2013).
8. Jain, R. K. & Stylianopoulos, T. Delivering nanomedicine to solid tumors. *Nat Rev Clin Oncol* **7**, 653–64 (2010).
9. Davis, M. E., Chen, Z. G. & Shin, D. M. Nanoparticle therapeutics: an emerging treatment modality for cancer. *Nat. Rev. Drug Discov.* **7**, 771–82 (2008).
10. Peer, D. *et al*. Nanocarriers as an emerging platform for cancer therapy. *Nat Nanotechnol* **2**, 751–60 (2007).
11. Byrne, J. D., Betancourt, T. & Brannon-Peppas, L. Active targeting schemes for nanoparticle systems in cancer therapeutics. *Adv Drug Deliv Rev* **60**, 1615–26 (2008).
12. van der Meel, R., Vehmeijer, L. J., Kok, R. J., Storm, G. & van Gaal, E. V. Ligand-targeted particulate nanomedicines undergoing clinical evaluation: Current status. *Adv Drug Deliv Rev* **65**, 1284–1298 (2013).
13. Florence, A. T. "Targeting" nanoparticles: the constraints of physical laws and physical barriers. *J. Control. Release* **164**, 115–24 (2012).
14. Kirpotin, D. B. *et al*. Antibody targeting of long-circulating lipidic nanoparticles does not increase tumor localization but does increase internalization in animal models. *Cancer Res.* **66**, 6732–40 (2006).
15. Pirollo, K. F. & Chang, E. H. Does a targeting ligand influence nanoparticle tumor localization or uptake? *Trends Biotechnol.* **26**, 552–8 (2008).
16. Choi, C. H., Alabi, C. A., Webster, P. & Davis, M. E. Mechanism of active targeting in solid tumors with transferrin-containing gold nanoparticles. *Proc Natl Acad Sci U S A* **107**, 1235–40 (2010).
17. Gao, H. *et al*. Ligand modified nanoparticles increases cell uptake, alters endocytosis and elevates glioma distribution and internalization. *Sci Rep* **3**, 2534 (2013).
18. Mahmoudi, M., Azadmanesh, K., Shokrgozar, M. A., Journeay, W. S. & Laurent, S. Effect of nanoparticles on the cell life cycle. *Chem. Rev.* **111**, 3407–32 (2011).
19. Lesniak, A. *et al*. Effects of the presence or absence of a protein corona on silica nanoparticle uptake and impact on cells. *ACS Nano* **6**, 5845–57 (2012).
20. Zhang, H., Mardyani, S., Chan, W. C. & Kumacheva, E. Design of biocompatible chitosan microgels for targeted pH-mediated intracellular release of cancer therapeutics. *Biomacromolecules* **7**, 1568–72 (2006).
21. Jiang, W., Kim, B. Y., Rutka, J. T. & Chan, W. C. Nanoparticle-mediated cellular response is size-dependent. *Nat Nanotechnol* **3**, 145–50 (2008).
22. Kim, J. A., Aberg, C., Salvati, A. & Dawson, K. A. Role of cell cycle on the cellular uptake and dilution of nanoparticles in a cell population. *Nat Nanotechnol* **7**, 62–8 (2012).
23. Cheetham, P. & Petrylak, D. P. Tubulin-targeted agents including docetaxel and cabazitaxel. *Cancer J.* **19**, 59–65 (2013).
24. Payton, S. Prostate cancer: Timing is everything for docetaxel therapy. *Nat Rev Urol* **10**, 123 (2013).
25. Ramaswamy, B. & Puhalla, S. Docetaxel: a tubulin-stabilizing agent approved for the management of several solid tumors. *Drugs Today (Barc)* **42**, 265–79 (2006).

26. Gao, H. *et al.* Study and evaluation of Mechanisms of Dual Targeting Drug Delivery System with Tumor Microenvironment Assays Compared with Normal Assays. *Acta Biomater* **10**, 858–867 (2014).
27. Gao, H. *et al.* Whole-cell SELEX aptamer-functionalised poly(ethyleneglycol)-poly(epsilon-caprolactone) nanoparticles for enhanced targeted glioblastoma therapy. *Biomaterials* **33**, 6264–72 (2012).
28. Miyoshi, N., Uchida, K., Osawa, T. & Nakamura, Y. A link between benzyl isothiocyanate-induced cell cycle arrest and apoptosis: involvement of mitogen-activated protein kinases in the Bcl-2 phosphorylation. *Cancer Res.* **64**, 2134–42 (2004).
29. Emanuel, S. *et al.* The in vitro and in vivo effects of JNJ-7706621: a dual inhibitor of cyclin-dependent kinases and aurora kinases. *Cancer Res.* **65**, 9038–46 (2005).
30. Li, F. *et al.* Control of apoptosis and mitotic spindle checkpoint by survivin. *Nature* **396**, 580–4 (1998).
31. Stenseth, K. & Thyberg, J. Monensin and chloroquine inhibit transfer to lysosomes of endocytosed macromolecules in cultured mouse peritoneal macrophages. *Eur. J. Cell Biol.* **49**, 326–33 (1989).
32. Lamaze, C. & Schmid, S. L. The emergence of clathrin-independent pinocytic pathways. *Curr. Opin. Cell Biol.* **7**, 573–80 (1995).
33. de Carcer, G., Perez, D. C. I. & Malumbres, M. Targeting cell cycle kinases for cancer therapy. *Curr. Med. Chem.* **14**, 969–85 (2007).
34. Schwartz, G. K. & Shah, M. A. Targeting the cell cycle: a new approach to cancer therapy. *J. Clin. Oncol.* **23**, 9408–21 (2005).
35. Kim, S. Y., Lee, Y. M., Baik, D. J. & Kang, J. S. Toxic characteristics of methoxy poly(ethylene glycol)/poly(epsilon-caprolactone) nanospheres; in vitro and in vivo studies in the normal mice. *Biomaterials* **24**, 55–63 (2003).
36. Mitchison, T. & Kirschner, M. Dynamic instability of microtubule growth. *Nature* **312**, 237–42 (1984).
37. Murray, J. W. & Wolkoff, A. W. Roles of the cytoskeleton and motor proteins in endocytic sorting. *Adv Drug Deliv Rev* **55**, 1385–403 (2003).
38. Rogers, S. L. & Gelfand, V. I. Membrane trafficking, organelle transport, and the cytoskeleton. *Curr. Opin. Cell Biol.* **12**, 57–62 (2000).
39. Yvon, A. M., Wadsworth, P. & Jordan, M. A. Taxol suppresses dynamics of individual microtubules in living human tumor cells. *Mol. Biol. Cell* **10**, 947–59 (1999).
40. Aniento, F., Emans, N., Griffiths, G. & Gruenberg, J. Cytoplasmic dynein-dependent vesicular transport from early to late endosomes. *J. Cell Biol.* **123**, 1373–87 (1993).
41. Lemasters, J. J. *et al.* Role of mitochondrial inner membrane permeabilization in necrotic cell death, apoptosis, and autophagy. *Antioxid Redox Signal* **4**, 769–81 (2002).
42. Kroemer, G., Galluzzi, L. & Brenner, C. Mitochondrial membrane permeabilization in cell death. *Physiol. Rev.* **87**, 99–163 (2007).
43. Fu, Q. *et al.* Nanoparticle albumin-bound (NAB) technology is a promising method for anti-cancer drug delivery. *Recent Pat Anticancer Drug Discov* **4**, 262–72 (2009).
44. Damascelli, B. *et al.* Intraarterial chemotherapy with polyoxyethylated castor oil free paclitaxel, incorporated in albumin nanoparticles (ABI-007): Phase II study of patients with squamous cell carcinoma of the head and neck and anal canal: preliminary evidence of clinical activity. *Cancer* **92**, 2592–602 (2001).
45. Sadauskas, E. *et al.* Kupffer cells are central in the removal of nanoparticles from the organism. *Part Fibre Toxicol* **4**, 10 (2007).
46. Gao, H. *et al.* A cascade targeting strategy for brain neuroglial cells employing nanoparticles modified with angiopep-2 peptide and EGFP-EGF1 protein. *Biomaterials* **32**, 8669–8675 (2011).

Acknowledgments

We thank Dr. Lixin Wu (Shanghai Pharma Engine Co., Ltd.) for technical assistance with flow cytometry. This work was supported by the National Basic Research Program of China (973 Program, 2013CB932504) National Natural Science Foundation of China (81072599).

Author contributions

H.G., X.J. and Q.H. conceived the experiment, designed the project and wrote the paper. H.G. performed the experiments with the assistance of G.H., Q.Z. and S.Z.

Additional information

Supplementary information accompanies this paper at http://www.nature.com/scientificreports

Competing financial interests: The authors declare no competing financial interests.

How to cite this article: Gao, H.L. *et al.* Pretreatment with chemotherapeutics for enhanced nanoparticles accumulation in tumor: the potential role of G2 cycle retention effect. *Sci. Rep.* **4**, 4492; DOI:10.1038/srep04492 (2014).